Valence and diffuse-bound anions of noble-gas complexes with uracil

Cite as: J. Chem. Phys. **137**, 194310 (2012); https://doi.org/10.1063/1.4766735
Submitted: 27 August 2012 . Accepted: 25 October 2012 . Published Online: 21 November 2012

Lívia Streit, O. Dolgounitcheva, V. G. Zakrzewski, and J. V. Ortiz

Valence and diffuse-bound anions of noble-gas complexes with uracil

Lívia Streit, O. Dolgounitcheva, V. G. Zakrzewski, and J. V. Ortiz[a)]
Department of Chemistry and Biochemistry, Auburn University, Auburn, Alabama 36849–5312, USA

(Received 27 August 2012; accepted 25 October 2012; published online 21 November 2012)

Valence-bound (VB) and diffuse-bound (DB) anions of noble-gas (Ar, Kr, and Xe) complexes with uracil have been studied with *ab initio* methods. MP2 optimizations revealed minima corresponding to anions of both kinds in each case. Coupled-cluster singles and doubles with perturbative triples, CCSD(T), and electron propagator single-point calculations were performed in order to assess vertical and adiabatic electron detachment energies of these complexes. *Ab initio* electron propagator calculations employed the outer valence Green's function and partial third-order approximations, and the algebraic diagrammatic construction in third order. Basis set effects have been systematically examined. DB anions of all three complexes were adiabatically bound, with calculated adiabatic electron attachment energies below 0.06 eV. Corresponding vertical electron detachment energies were below 0.1 eV. As to VB anions, only the Xe complex had a positive adiabatic electron detachment energy, of 0.01 eV, with a corresponding vertical electron detachment energy of 0.6 eV. These computational findings are consistent with the interpretation of results previously obtained experimentally by Hendricks *et al.* © *2012 American Institute of Physics*. [http://dx.doi.org/10.1063/1.4766735]

I. INTRODUCTION

Purine and pyrimidine anions play an important role in biochemistry, for they are known as intermediates of radiation-induced reactions that can lead to permanent damage of genetic material. Nucleic acid base (NAB) anions are created when free electrons resultant from these reactions are trapped by nucleobases, creating anionic species. NAB anions' chemistry thus would provide relevant information to understanding DNA and RNA mutagenesis.[1–3]

The formation of NAB anions can be due to the attachment of an electron to either a valence molecular orbital, or to a diffuse orbital that is slightly displaced from the nuclear structure. Species known as valence-bound anions comprise the former group. In this case, neutral and anionic structures exhibit different geometries and an extra electron is expected to be strongly bound. Usually, the valence molecular orbital of a neutral parent is of the π type. In the latter case, the diffuse-bound anions present small electron detachment energies, for the excess electron is weakly bound by the neutral. Structures of diffuse-bound anions are virtually the same as those of the corresponding neutrals and the MO in question is of the σ type.

The formation of unstable anions of purines and pyrimidines was first reported by Anbar and St. John[4] in 1975 for thymine. The first computational prediction of an adiabatically bound anion of uracil was made by Oyler and Adamowicz.[5] In this work, the authors demonstrated that additional diffuse functions were necessary to predict positive electron affinities corresponding to diffuse-bound (DB) purine and pyrimidine anions. A positive adiabatic electron affinity (AEA) was obtained for uracil at the MP2/6-31+G*X (in which X is the additional set of diffuse functions with optimized exponents) level of theory. Computational predictions of Oyler and Adamowicz[5] motivated subsequent experimental investigations. Photoelectron experiments have characterized both uracil and thymine anions as fragile, weakly bound species with vertical electron detachment energies (VEDEs) below 0.1 eV.[6–8] A pioneering study on the DB to valence-bound (VB) anion transformation in uracil was reported by Hendricks *et al.* in 1998.[8] In that study, photoelectron experiments for uracil anion showed a sharp and intense peak between 0 and 0.1 eV characterizing the existence of a weakly bound species, interpreted as DB anions, in which the anion presented practically the same structure as its parent neutral. The transformation of the DB anion to a VB anion was observed when uracil anions coordinated to a xenon atom or water molecule were studied and the sharp, intense peak in the spectrum was replaced in some cases by a broad, widely spread band. Complexes such as $U^-(H_2O)$, $U^-(Ar)$, $U^-(Kr)$, and $U^-(Xe)$ were considered. Figure 1 reproduces spectra of the uracil anion complexes.

The authors thus have concluded that the uracil DB anion gradually changes to a VB anion as the interaction with the coordinating species becomes stronger. In other words, a water molecule, or a Xe atom, suffice to stabilize a VB anion, but neither Ar nor Kr is able to cause the diffuse-to-valence bound anion transformation.

Complexes of nucleobases such as thymine, cytosine, adenine, and uracil with water are still widely studied and constitute a useful model for studying the binding transformation between the DB and VB anions. Motivated by the realization that NAB anions form VB species in biologically condensed-phase environments,[7,9,10] computational predictions of VEDEs and AEAs for uracil-water complexes have been made with several levels of quantum chemical methods, such as second-order many-body perturbation theory (MBPT2 or MP2),[11–13] coupled cluster,[14,15]

[a)]Electronic mail: ortiz@auburn.edu.

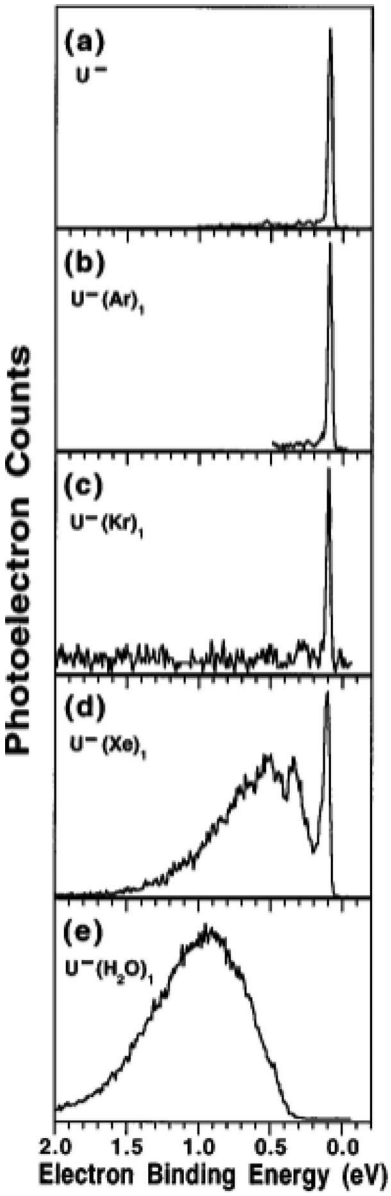

FIG. 1. Photoelectron spectra recorded using 2.540 eV photons: (a) the photoelectron spectrum of the uracil anion, U^-, (b) the photoelectron spectrum of the uracil anion coordinated to an argon atom, $U^-(Ar)$; (c) the photoelectron spectrum of the uracil anion coordinated to a krypton atom, $U^-(Kr)$; (d) the photoelectron spectrum of the uracil anion coordinated to a xenon atom, $U^-(Xe)$; (e) the photoelectron spectrum of the uracil anion coordinated to a water molecule, $U^-(H_2O)$. Reprinted with permission from Hendricks *et al.*, J. Chem. Phys. **108**, 8 (1998). Copyright 1998 American Institute of Physics.

multiconfigurational perturbative methods (such as CASPT2),[14] and density functional theory (DFT).[16–18] Except for the DFT method, which has been shown to overestimate AEAs by approximately 0.3 eV, *ab initio* theoretical data can provide information to explain the existence of $U^-(H_2O)_n$ VB anions. Conversely, interaction of the uracil anion with noble-gas atoms has not been widely explored. Motivated by the work of Hendricks *et al.*,[8] Jalbout *et al.*[19] have investigated, with the MP2/6-31++G** level of theory, two models of interaction of the uracil anion with closed-shell systems: an argon atom and a nitrogen molecule. In that study, the authors have found that neither U(Ar) nor $U(N_2)$

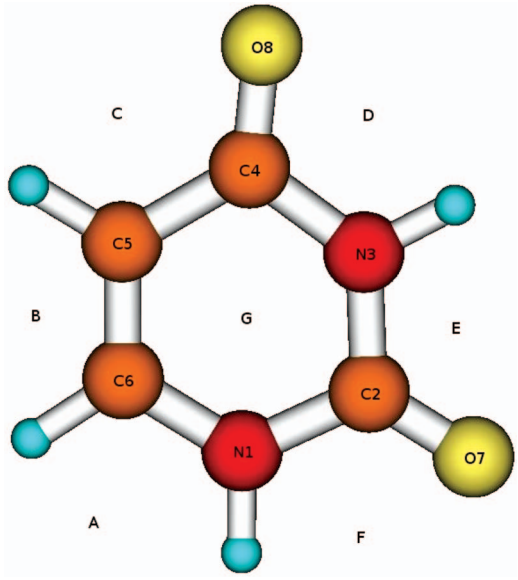

FIG. 2. Uracil numbering and labeling schemes.

forms stable anions when the interacting species is placed close to the DB anion's singly occupied orbital. In contrast, when the argon atom or nitrogen molecule is placed on the opposite side of the diffuse orbital in the uracil anion, both systems form vertically and adiabatically stable DB anions.

More recently, theoretical studies of tautomers of NBAs such as uracil, adenine, and guanine have been published.[20–22] Bachorz *et al.*[20] have shown that the most stable anion of uracil is related to an imino-oxo tautomer, in which one N1-bound proton is transferred to the C5 atom (U_{C5N1}), see Figures 2 and 10. This tautomer, as well as U_{C6N1} and U_{C5N3} structures, were called "very rare tautomers" of uracil. The U, VB anion is characterized by a VEDE of 1.27 eV and is adiabatically stable with respect to the canonical neutral by 3.93 kcal/mol. It is also more stable than the DB or VB anions of the canonical tautomer by 2.32 and 5.10 kcal/mol, respectively.

In the current work, we attempt to characterize both DB and VB anions of U(Ar), U(Kr), and U(Xe) complexes and to describe the species that are observed in the photoelectron experiments.[8] Very rare tautomers of uracil rare-gas complexes also are studied. AEAs and VEDEs are determined with electron propagator theory,[23,24] many-body perturbation theory and coupled-cluster theory. Practical calculations using MP2, and CCSD(T) have been done using the GAUSSIAN 09 package.[25] Quasiparticle propagator calculations have done using codes incorporated in G09 (with algorithms described in Refs. 26–28). Third-order algebraic diagrammatic construction ADC(3) electron propagator calculations[29–32] were performed with a modified version of G09.

II. METHODS

AEAs of U(Ar), U(Kr), and U(Xe) complexes of their VB and DB anions are investigated with many-body perturbation and coupled cluster theories. VEDEs and VEAEs (vertical electron attachment energies) of the anions were also calculated with electron propagator theories.[23,24]

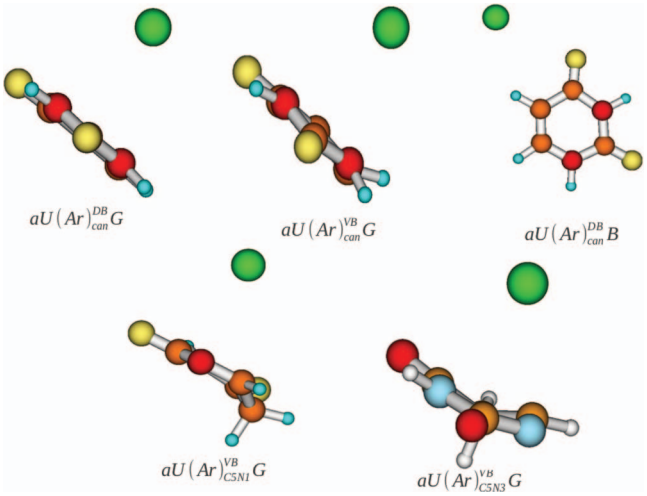

FIG. 3. Optimized geometries of U(Ar) canonical aB and aG anions, C5N1 and C5N3 aG anions.

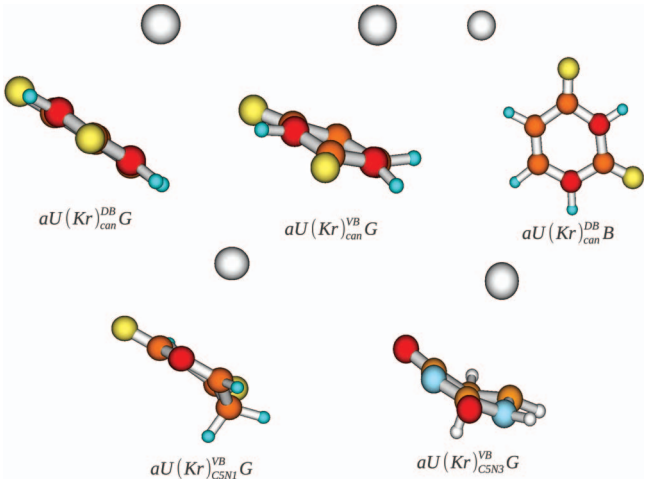

FIG. 5. Optimized geometries of U(Kr) canonical aB and aG anions, C5N1 and C5N3 aG anions.

A. Computational details

Initial optimizations of the uracil-noble gas (U · NG) complexes were performed with MP2 and the 6-311G** basis on uracil and Ar. For U · Kr and U · Ar complexes, aug-cc-pVDZ basis sets with effective core potentials (aug-cc-pVD(Q)Z-PP) on the krypton and xenon atoms[33] were used. Seven positions of a noble-gas atom about uracil moiety were chosen for initial MP2/6-311G** optimizations of neutral U · NG complexes. Of these, six configurations, labelled as A, B, C, D, E, and F, were planar whereas the seventh configuration (G) had an above-plane position for the NG atom (see Figure 2). The structures obtained in this way and the corresponding DB and VB anions (denoted as aA to aG) were reoptimized with MP2 and 6-311++G**. Geometry optimizations have converged to the structures shown in Figures 3–5. In order to verify minima, harmonic frequency calculations were performed for all optimized configurations. At this point, only two configurations, namely, B and G, were confirmed minima. None of the anions were bound at this level of theory. To obtain bound DB anions, additional diffuse functions were needed. According to Dolgounitcheva *et al.*,[11] addition of another set of diffuse *s* and *p* functions is extremely important for describing diffuse-bound uracil anions. *s* and *p* functions for O, N, and C atoms are generated by dividing the exponents of the most diffuse functions of the 6-311++G** basis by three. *s* and *p* functions with 0.001 exponents on each hydrogen atom also are added. The resulting basis set designated B2 (Ref. 11) was used to evaluate total electronic energies of the minima previously obtained at the UMP2/6-311++G** level of theory.

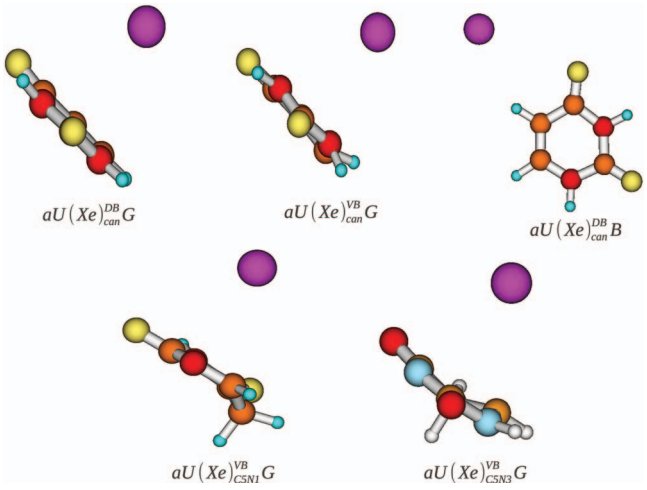

FIG. 4. Optimized geometries of U(Xe) canonical aB and aG anions, C5N1 and C5N3 aG anions.

Harmonic frequency calculations were carried out for all optimized structures obtained at the MP2/6-311++G** level. Some of the structures were reoptimized with the B2 basis. Since the ZPE corrections remained virtually the same with the change of basis set, ZPE corrections obtained at the MP2/6-311++G** level of theory were employed for calculating AEAs at the MP2/B2 level of theory. VB anions were reoptimized with the aug-cc-pVDZ basis.[34,35] Harmonic frequency calculations also were carried out at this level.

Although the MP2 method includes some correlation effects and is not a computationally demanding alternative, highly correlated methods are necessary for accurate AEAs and VEDEs results. Therefore, coupled-cluster singles and doubles with perturbative triples, or CCSD(T), electronic energies were obtained with 6-311++G(2df,2dp), 6-311++G(3df,2p), and aug-cc-pVDZ basis sets. Additional diffuse functions were included by the same procedure. Finally, single-point CCSD(T)/aug-cc-pVQZ calculations were performed on the aug-cc-pVDZ optimized VB anions and the corresponding neutrals.

The electron propagator theory[23,24] is a computationally economic and accurate method for calculating VEDEs and VEAEs. The outer valence Green's function (OVGF) and partial third order (P3) approximations include orbital relaxation and electron correlation effects, providing very accurate VEDE values. VEDEs of anions were calculated with the OVGF and P3 approximations and the B2 basis set for DB anions; the 6-311++G** basis set was used for VB anions. Similarly, VEAEs of neutral molecules are obtained with the ADC(3) method. VEAEs were calculated for the

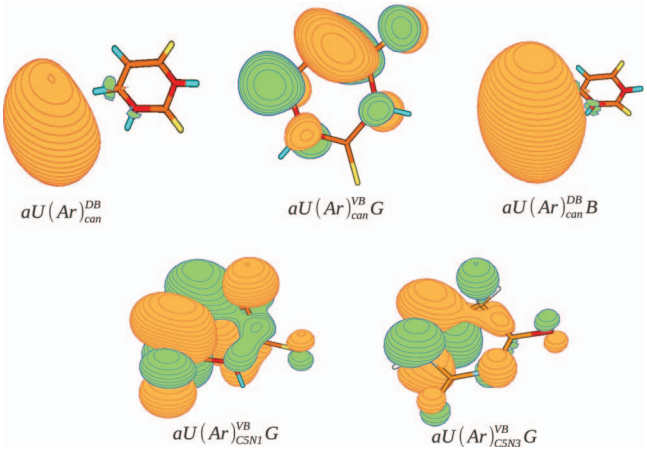

FIG. 6. Molecular diagrams of U(Ar) canonical aB and aG anions, C5N1 and C5N3 aG anions.

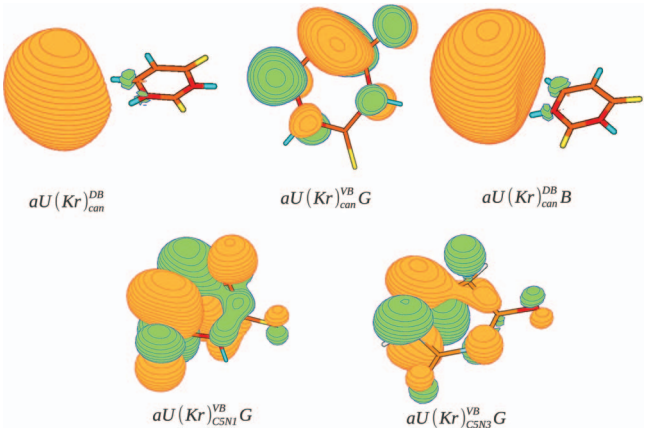

FIG. 8. Molecular diagrams of U(Kr) canonical aB and aG anions, C5N1 and C5N3 aG anions.

neutral structures with the ADC(3) method and the B2 basis set. A brief outline of electron propagator theory is presented in Sec. II B.

All calculations were performed with the GAUSSIAN 09 (Ref. 25) package and all figures were produced with Molden 5.0.[36] Orbital pictures (Figures 6–8) were created by considering isosurface values of 0.04 and 0.01 for the VB and DB structures, respectively.

B. Electron propagator methods

Electron propagator calculations of vertical electron detachment and attachment energies are based on the Dyson equation.[23,37] The Dyson equation is written in the form of one-electron equations such that

$$[\hat{f} + \hat{\Sigma}(\varepsilon_i)]\phi_i^{Dyson}(x) = \varepsilon_i \phi_i^{Dyson}(x), \quad (1)$$

where $\hat{f}$ is the Fock operator and $\hat{\Sigma}(\varepsilon)$ is an energy-dependent nonlocal operator, the self-energy, which describes electron correlation and orbital relaxation effects. For each VEDE, there corresponds a Dyson orbital, $\phi_i^{Dyson}(x)$, defined by

$$\phi_i^{Dyson}(x_1) = \sqrt{N} \int \Psi_N(x_1, x_2, x_3, \ldots, x_N) \times \Psi^*_{i,N-1}(x_2, x_3, \ldots, x_N) dx_2 \ldots dx_N, \quad (2)$$

where N is the number of electrons in the initial state and x_r is the space-spin coordinate of electron r. $\Psi_N(x_1, \ldots, x_N)$ is the wavefunction for the N-electron initial state and $\Psi_{i,N-1}(x_2, \ldots, x_N)$ is the wavefunction for the ith final state with $N-1$ electrons. The eigenvalues ε_i correspond to electron binding energies.

The most commonly used types of electron propagator approximations are the OVGF and P3. Both of them neglect off-diagonal elements of the self-energy matrix, where differential correlation and orbital relaxation corrections are included, in the canonical, Hartree-Fock basis. OVGF and P3 methods involve the evaluation of third-order terms in the self-energy. In the diagonal approximation, the Dyson equation has a simple form

$$E_p = \varepsilon_p + \Sigma_{pp}(E_p), \quad (3)$$

where the self-energy matrix is designated by $\Sigma(E)$ and ε_p is a canonical, Hartree-Fock energy. The pole strength (PS) associated with a given binding energy is related to the corresponding Dyson orbital by

$$P_q = \int |\phi_q^{Dyson}(x)|^2 dx. \quad (4)$$

The PS is a good indicator of the qualitative validity of this approximation: PSs between 0.85 and unity indicate that the one-electron descriptions of final states, e.g., Koopmans's theorem, are qualitatively valid and that methods such OVGF and P3 are applicable. When PSs are less than 0.85, nondiagonal analysis of energy poles is required.[30]

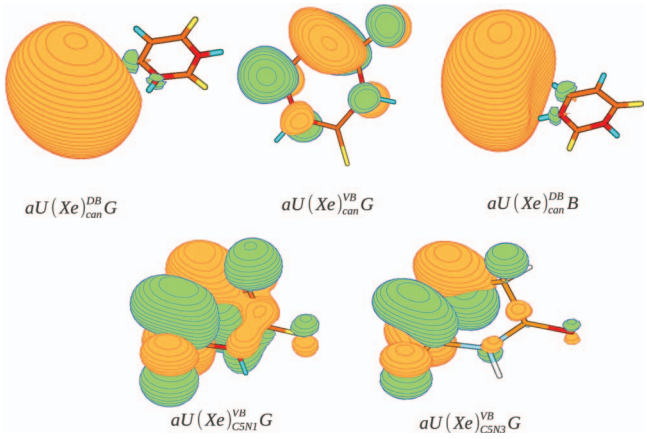

FIG. 7. Molecular diagrams of U(Xe) canonical aB and aG anions, C5N1 and C5N3 aG anions.

III. RESULTS AND DISCUSSION

The results obtained in the present work are presented in three sections. Energies at the optimized geometries obtained for the structures A to G (and DB anions aA to aG), as shown in Figure 2, for U(Ar), U(Kr), and U(Xe) complexes are

TABLE I. MP2 and PUMP2/6-311++G** total energies (a.u.) of the neutrals B and G, and the DB anions aB and aG.

Neutral	MP2	Anion	UMP2	PUMP2
U(Ar)				
B	−940.80580	aB	−940.79103	−940.79106
G	−940.80780	aG	−940.79277	−940.79280
U(Kr)				
B	−876.17540	aB	−876.17125	−876.17126
G	−876.17765	aG	−876.17419	−876.17420
U(Xe)				
B	−742.26863	aB	−742.25442	−742.25445
G	−742.27133	aG	−742.25675	−742.25678

discussed in Sec. III A. Table I summarizes such information. Total electronic energies for the minima previously obtained are presented in Sec. III B. DB and VB anions are identified, as shown in Table II. AEAs, VEDEs, and VEAEs are shown in Tables IV–VI and discussed in Sec. III C. These theoretical results are compared with experimental spectra.

Following the discussion for the canonical U(NG) anions, a study concerning complexes of very rare uracil tautomers with the noble-gas atoms is presented. The relevance of such study is justified throughout this section.

A. Structures

Six structures were investigated for U(Ar) and U(Xe) complexes. Initially, the noble-gas atom was placed in the uracil plane, according to Figure 2.

TABLE II. U(NG) and DB U^-(NG) MP2 and UMP2/B2 total energies (a.u.).

Structure	MP2	PUMP2
U(Ar)		
B	−940.80774	
B[a]	−940.80662	
aB	−940.80846	−940.80846
G	−940.81026	
G[a]	−940.80910	
aG	−940.81085	−940.81085
U(Kr)		
B	−876.17733	
B[a]	−876.17693	
aB	−876.17861	−876.17861
G	−876.17986	
G[a]	−876.17951	
aG	−876.18109	−876.18109
U(Xe)		
B	−742.27076	
B[a]	−742.26957	
aB	−742.27163	−742.27163
G	−742.27368	
G[a]	−742.27254	
aG	−742.27434	−742.27434

[a]Energies of the neutral structures at the anion geometry.

In addition, a seventh structure was studied, with the noble-gas atom placed above the ring. Geometry optimizations at the MP2/6-311++G** level of theory for U(Ar) and the MP2/6-311++G**/aug-cc-pVDZ-PP level of theory for U(Xe) and U(Kr) complexes converged to structures with total electronic energies presented in Table I.

Frequency calculations on the optimized geometries have shown four minima for U(Ar), structures B and aB, G and aG. These structures have C_1 symmetry, whereas structures A, C, D, and E (and their anions) were found with C_s symmetry. Structures F and aF have C_1 symmetry but are not minima. Structures D, E and aD, aE converged to structures with exactly the same geometry and therefore were named D and aD. The B complex and the anion aB optimized geometries are more similar to the initial geometries of C and aC than to original B and aB geometries. Deviations from planarity were measured according to the largest absolute dihedral angle (φ). In the B complex, deviations from planarity ($\varphi_{\text{C4-N3-C2-N1}}$) are as large as 11° for the neutral and not greater than 9° for the anion. The anion aB exhibited a greater deviation from planarity for the Ar atom with respect to the uracil ring of approximately 4° ($\varphi_{\text{N3-C4-O8-Ar}}$). The geometries of the neutral molecule and the anion are virtually the same, except for the slight modification in the Ar atom position, as shown in Figure 3.

When the Ar atom was placed above the uracil ring, the neutral G was found to be 1.26 kcal/mol more stable than B and aG was found 1.09 kcal/mol more stable than aB. Deviations from planarity of the uracil are around 11° for the neutral molecule and the anion ($\varphi_{\text{C4-N3-C2-N1}}$). The Ar atom is located 3.46 Å from the C6 atom in the neutral G and 3.51 Å in the anion aG, see Figure 3.

U(Xe) total electronic energies obtained at the MP2/6-311++G**/aug-cc-pVDZ-PP level of theory are shown in Table I. The same pattern as in U(Ar) geometry tendencies was observed for U(Xe). Four minima were also obtained, structures B and aB, G and aG, except that in the U(Xe) case, only non-planar structures are minima. G and aG are more stable than B and aB by 1.43 and 1.46 kcal/mol, respectively. All the structures other than the minima had C_s symmetry. Geometries of B, aB, G, and aG structures are shown in Figure 4.

The main differences between U(Ar) and U(Xe) geometries are related to G and aG structures. U(Xe) B and aB complexes showed almost the same geometric parameters as B and aB U(Ar) complexes. For U(Xe), the G structures present a deviation from planarity ($\varphi_{\text{C4-N3-C2-N1}}$) for the uracil ring as large as 13°, and for the aG structure, 9°. The Xe atom is placed 3.72 Å from the C6 atom in both structures. For U(Kr) complexes, only the B and G structures were studied, since the experimental work of Hendricks *et al.*[8] showed the same spectral pattern for the U(Ar) complex. In Table I, the total electronic energies obtained for the optimized structures B, aB, G, and aG at the MP2/6-311++G**/aug-cc-pVDZ-PP level of theory are shown. G and aG were found as minima. Figure 5 shows the optimized geometries of G and aG structures. Deviations from planarity ($\varphi_{\text{C4-N3-C2-N1}}$) of 10° and 9° with respect to the uracil ring were found for G and aG, respectively.

TABLE III. U(NG) and VB U^-(NG) UMP2/6-311++G** and aug-cc-pVDZ and CCSD(T)/aug-cc-pVDZ ZPE corrected total energies (a.u.)

	UMP2		
Structure	6-311++G**	aug-cc-pVDZ	CCSD(T)
U(Ar)			
G	−940.723146	−940.650728	−940.744380
aG	−940.712835	−940.648056	−940.743070
U(Kr)			
G	−876.092987	−876.020858	−876.110821
aG	−876.083553	−876.018885	−876.110151
U(Xe)			
G	−742.186637	−742.114656	−742.203277
aG	−742.178509	−742.113789	−742.203616

VB anions were found for aG structures for the three uracil-noble gas complexes. Uracil geometries in U^-Ar, U^-Kr, and U^-Xe are essentially the same. No significant increase of non-planarity or ring puckering from U(Ar) to U(Xe) was observed. Ring puckering was shown to be mostly due to deviation from planarity by N_1 with the dihedral angle H-C_5-C_6-N_1 approximately 5° out of the plane. The optimized geometries at the UMP2/aug-cc-pVDZ level of theory showed larger deviations from planarity of approximately 11° ($\varphi_{C4\text{-}N3\text{-}C2\text{-}N1}$) for all three VB aG complexes.

B. Energies and molecular orbitals

Total energies for neutral and DB anionic species found as minima of U(Ar), U(Xe), and U(Kr) at the MP2/B2 level of theory are given in Table II. Total energies for VB anionic species (ZPE corrected) at MP2/6-311++G**, MP2/aug-cc-pVDZ, and CCSD(T)/aug-cc-pVDZ levels of theory are shown in Table III.

1. DB anions

The anions studied in Sec. II were identified as DB anions by inspection of the optimized geometries (neutral and anionic species present virtually the same geometry). This idea was confirmed with the analysis of orbital graphs. Inclusion of additional diffuse functions decreased anionic electronic energies, yielding DB anions that were adiabatically bound with respect to the neutral.

For the U(Ar) case, aB and aG DB anions are adiabatically bound by 0.020 and 0.016 eV, respectively. Considering the ZPE corrections, the aB anion is adiabatically unbound with respect to the neutral by 0.002 eV, whereas the aG anion is bound by 0.035 eV. Those structures showed almost no spin contamination (see Table II). After projection of quartet contaminants, the electronic energies were only slightly modified and before projection, $\langle s^2\rangle_{UHF}$ values were very close to 0.75. Figure 6 shows a diffuse singly occupied orbital for the aB and aG anions.

For U(Xe), two DB anions were found. aB and aG DB anions are adiabatically bound with respect to the neutrals by 0.024 and 0.018 eV, respectively. When the ZPE corrections are considered aB and aG DB anions are both adiabatically bound by 0.046 and 0.044 eV. Orbital plots presented in Figure 7 show singly occupied orbitals with diffuse lobes that are characteristic of DB anions.

For the U(Kr) complex, aB and aG DB anions are adiabatically bound with respect to the neutrals by 0.035 and 0.033 eV, respectively. When ZPE corrections are incorporated, those values become 0.046 and 0.040, respectively. The diffuse singly occupied orbitals for the aB and aG anions are shown in Figure 8.

2. VB anions

VB anions related to the G structure were obtained and their electronic energies calculated at the UMP2/6-311++G** level of theory are shown in Table III.

The optimized geometry of U^-(Ar) is presented in Figure 3 and the orbital picture is shown in Figure 6. The large deviation from planarity and consequently, the large difference between the neutral and VB anionic species suggests this structure is a VB anion. The orbital picture (see Figure 6), depicts the localized lobes that characterize valence orbitals. DB anions typically present $\langle s^2\rangle_{UHF}$ values close to 0.75 because the singly occupied molecular orbital has little spatial overlap with the other occupied molecular orbitals. Therefore, the $\langle s^2\rangle_{UHF}$ value of 0.80, confirms the inference of the existence of a VB anion. The aG VB anion of U(Ar) is adiabatically unbound with respect to the neutral G by 0.287 eV and by 0.315 eV when ZPE corrections are considered, at the PUMP2 level of theory. At the CCSD(T)/6-311++G(2df,2p) level of theory, the aG VB anion is unbound with respect to the neutral G by 0.531 eV and 0.458 eV when ZPE corrections are considered.

For the U(Xe) complex, a VB anion that is adiabatically unbound with respect to the neutral G by 0.230 eV was found. This value is reduced to 0.160 eV with the incorporation of ZPE corrections at the PUMP2 level of theory. The optimized geometry is presented in Figure 4. Additionally, another VB anion was found as a minimum, starting at the geometry of the aB DB anion. The optimized geometry, is very close to the aG VB anion, and it therefore was named aG′. The aG′ VB anion is less stable than aG VB anion by 0.17 kcal/mol and is adiabatically unbound with respect to the neutral G by 0.163 eV (energies are ZPE corrected). Since the two VB anions have practically the same energy and present the same AEA value, one can assume that both structures coexist. The structures G and aG were reoptimized using the Dunning basis set aug-cc-pVDZ on the uracil molecule at the UMP2 level of theory. At this level, the VB aG U(Xe) anion is still adiabatically unbound with respect to the neutral. However, the relative energy value is decreased to 0.122 and 0.023 eV when ZPE corrections are considered. Total electronic energies were calculated for the structures thus obtained at the UMP2/aug-cc-pVQZ level of theory. At this level, the VB aG U(Xe) anion was found *adiabatically bound* with respect to the parent neutral by 0.075 eV when ZPE corrections were considered. Additional *s*, *p*, and *d* diffuse functions on the Xe atom were also considered. At the PUMP2/6-311++G** level of theory, the AEA ZPE corrected value for the aG VB U(Xe) anion is

TABLE IV. U(NG) VB aG PUMP2 and CCSD(T) AEAs (ZPE corrected) (eV) with aug-cc-pVDZ and aug-cc-pVQZ basis sets.

Method	Basis set	U(Ar)	U(Kr)	U(Xe)
UMP2	aug-cc-pVDZ	−0.073	− 0.0537	− 0.024
	aug-cc-pVQZ	[a]	0.027	0.075
CCSD(T)	aug-cc-pVDZ	−0.036	− 0.020	0.010

[a]Calculations did not converge for the anion with the aug-cc-pVQZ basis set.

−0.156 eV when extra diffuse *s*, *p*, and *d* functions of exponents 0.01, 0.01, and 0.1, respectively, are incorporated to the aug-cc-pVDZ-PP basis set. This value is practically the same, −0.160 eV, when the aug-cc-pVTZ-PP basis set is used on Xe atom.

At the CCSD(T) level with the 6-311++G(2df,2p) basis set on uracil molecule, the VB aG U(Xe) anion is unbound with respect to the neutral by 0.061 eV. With the 6-311++G(3df,2p) basis set and considering ZPE corrections, this value is reduced to 0.003 eV. The tendency of decreasing AEA values with improving basis sets on uracil evinces that the diffuse *d* functions on uracil are important in describing the VB anion. Therefore, CCSD(T) total electronic energies were obtained with the aug-cc-pVDZ basis set on uracil. ZPE corrected total electronic energies obtained at that level of theory are also shown in Table III. Table IV summarizes the AEA values obtained with Dunning basis sets for the aG VB U(NG) anions.

At the CCSD(T) level of theory, the VB aG U(Xe) anion was found *adiabatically bound* with respect to the neutral by 0.01 eV (ZPE corrected).

The U^-(Kr) VB complex presented the same qualitative results as the U^-(Ar) VB complex. The optimized geometry of U^-(Ar) is presented in Figure 5 and the orbital picture is shown in Figure 8. An aG VB anion adiabatically unbound with respect to the neutral by 0.266 eV (0.196 eV when ZPE corrected) was found. At the CCSD(T)/6-311++G(2df,2p)/aug-cc-pVDZ-PP level of theory, that value is decreased to 0.491 eV. The structures G and aG of the U(Kr) complex were reoptimized at the UMP2/aug-cc-pVDZ level of theory, resulting in an aG VB anion that is adiabatically unbound with respect to the neutral by 0.054 eV, with ZPE corrections. Total electronic energies were calculated for the structures thus obtained at the UMP2/aug-cc-pVQZ level of theory. At this level, the aG VB U(Kr) anion was found adiabatically bound with respect to the parent neutral by 0.027 eV.

At the CCSD(T) level with the aug-cc-pVDZ basis set on the uracil molecule, the aG VB U(Kr) anion was found adiabatically unbound with respect to the neutral by 0.020 eV (ZPE corrected). The graphic shown in Figure 9 compares the CCSD(T) relative energies for the U(NG) VB anions and identifies the U(Xe) VB anion as the only adiabatically bound complex. The relative energies shown in Figure 9 were calculated at CCSD(T)/6-311++G(2df,2p)//UMP2/6-311++G(d,p), CCSD(T)/6-311++G(3df,2p)//UMP2/6-311++G(d,p), and CCSD(T)/aug-cc-pVDZ//UMP2/aug-cc-pVDZ levels of theory.

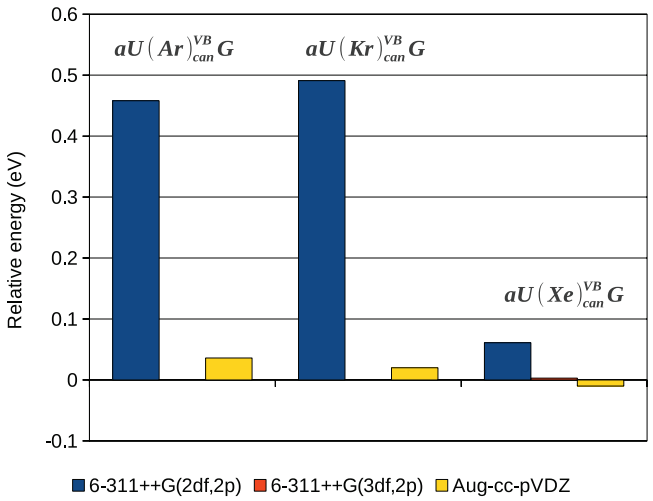

FIG. 9. Relative energies (ZPE corrected) for the U(NG) VB anions with respect to the canonical neutral (eV) at the CCSD(T) level of theory.

C. AEAs and VEDEs

1. DB anions

AEAs for all the U(NG) (NG = Ar, Kr or Xe) complexes were calculated at the MP2, UMP2, and CCSD(T) levels of theory and are shown in Table V.

For the U(Xe) G/aG pair, UMP2/B2 geometries were reoptimized and ZPEs were calculated at the same level. The resulting ZPE corrections, 0.0870 and 0.0869 a.u., respectively, coincided with the UMP2/6-311++G** (or UMP2/6-311++G**/aug-cc-pVDZ) values. Therefore, for all isomers, ZPEs at the UMP2/6-311++G** were incorporated into AEAs. At the UMP2/B2 level of theory, all the DB anions display positive AEAs at UMP2 and PUMP2 levels.

CCSD(T) calculations did not converge for the U^-(Kr) and U^-(Xe) anions with the B2 basis set (6-311++G**/aug-cc-pVDZ-PP with the additional diffuse functions). At the UMP2/B2 level of theory both aB and aG DB anions of U(Kr)

TABLE V. U(NG) UMP2/B2, PUMP2/B2, and CCSD(T)/B2 AEAs (eV).

		UMP2		PUMP2		CCSD(T)	
Structure		AEA	AEA+ZPE	AEA	AEA+ZPE	AEA	AEA+ZPE
U(Ar)							
B	DB	0.019	0.019	0.019	0.019	0.044	0.022
G	DB	0.016	0.034	0.016	0.034	0.037	0.056
	VB[a]	−0.398	−0.325	−0.287	−0.315	−0.531	−0.458
U(Kr)							
B	DB	0.035	0.046	0.035	0.046	[b]	[b]
G	DB	0.033	0.040	0.033	0.040	[b]	[b]
	VB[a]	−0.377	−0.307	−0.266	−0.196	−0.561	−0.491
U(Xe)							
B	DB	0.024	0.046	0.024	0.046	[b]	[b]
G	DB	0.018	0.043	0.018	0.043	[b]	[b]
	VB[a]	−0.341	−0.270	−0.230	−0.160	−0.135	−0.061
G′	VB[a]	−0.350	−0.275	−0.237	−0.163	−0.134	−0.061

[a]No additional diffuse functions were included. For CCSD(T) calculations, 6-311++G(2df,2p) basis set was used on uracil.
[b]CCSD(T) calculations did not converge with the B2 basis set.

TABLE VI. U^-(NG) UMP2, PUMP2, CCSD(T), OVGF and P3 VEDEs (eV), and ADC(3) VEAEs with the B2 basis set.

Structure		UMP2	PUMP2	CCSD(T)	OVGF	P3	ADC(3)
U(Ar)							
aB	DB	0.050	0.050	...	0.061	0.081	0.053
aG	DB	0.047	0.047	0.073	0.044	0.076	0.054
	VB[a]	0.276	0.387	0.563	0.534	0.767	...
U(Kr)							
aB	DB	0.046	0.046	[b]	0.068	0.073	0.047
aG	DB	0.043	0.043	[b]	0.024	0.068	0.047
	VB[a]	0.292	0.402	0.524	0.566	0.793	...
U(Xe)							
aB	DB	0.055	0.056	[b]	0.064	0.088	0.058
aG	DB	0.049	0.049	[b]	0.030	0.059	0.057
	VB[a]	0.260	0.371	0.609	0.593	0.824	...
aG′	VB[a]	0.252	0.363	0.610	0.593	0.824	...

[a]No additional diffuse functions were included. For CCSD(T) calculations, 6-311++G(2df,2p) basis set was used on uracil.
[b]CCSD(T) calculations did not converge with the B2 basis set.

and U(Xe) present positive AEAs, even when ZPE corrections are considered, in contrast with the U(Ar) aB DB anion.

OVGF, P3, and ADC(3) results are in good agreement with UMP2 values. According to Hendricks *et al.*,[8] U^-(Ar), U^-(Kr), and U^-(Xe) photoelectron spectra exhibit a sharp peak below 0.1 eV (see Figure 1) that is characteristic of VEDEs of weakly bound compounds in agreement with the values presented for the DB anions in Table VI. VEAEs values calculated at the ADC(3) level of theory for all the DB anions are also shown in Table VI. These values are in excellent agreement with the VEDEs calculated with MP2, OVGF and P3 methods and with experimental observations.

VEDE values calculated at the MP2, UMP2, CCSD(T), OVGF, and P3 levels of theory for all the DB anions are shown in Table VI. VEDE values of approximately 0.05 eV at MP2 and UMP2 levels of theory are in excellent agreement with spectra shown in Figure 1. OVGF VEDEs agree with MP2 and UMP2 results. P3 VEDEs as large as 0.8 eV were obtained. Nevertheless, P3 results are in excellent agreement with experimental observations.

2. VB anions

All the VB anions are adiabatically unbound with respect to the neutral, presenting negative AEA values and positive VEDEs at the UMP2, PUMP2, and CCSD(T) levels with the 6-311**G basis set. With the Dunning aug-cc-pVQZ basis set, the U(Xe) VB aG anion is adiabatically bound with respect to the neutral, presenting a positive AEA value of 0.075 eV. At the same level of theory, both U(Ar) and U(Kr) VB aG anions present negative AEA values of 0.073 and 0.054 eV, respectively (see Table IV). At the CCSD(T)/aug-cc-pVDZ level of theory, the U(Xe) VB aG anion shows an AEA value of 0.010 eV, whereas the U(Ar) VB aG anion shows an AEA value of −0.036 eV. These results confirm experimental observations, for U^-(Ar) and U^-(Kr) photoelectron spectra display only sharp peaks below 0.1 eV. No other bands are evident.

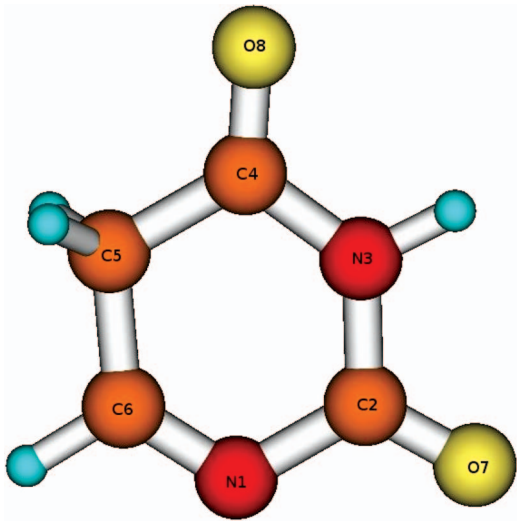

FIG. 10. Uracil C5N1 tautomer numbering and labeling schemes.

The U(Xe) spectrum in Figure 1 shows features that are charateristic of both DB and VB anions: a sharp peak below 0.1 eV and a broadband from 0.2 to 1.0 eV with a maximum about 0.5 eV. The results given in Table VI are in excellent agreement with the experimental data. U(Kr) and U(Ar) photoelectron spectra exhibit the same pattern: VB anions are not displayed, in agreement with the present work. Whereas U(Ar) and U(Kr) aG VB anions present AEA values as negative as −0.5 eV, the U(Xe) aG VB anion shows an AEA substantially closer to zero. This value becomes positive when the aug-cc-pVDZ basis set (aug-cc-pVQZ at the UMP2 level of theory) is used on uracil. U(Ar) G and aG structures, reoptimized at the UMP2/aug-cc-pVDZ level of theory, as well as electronic energies calculated at the UMP2/aug-cc-pVQZ and CCSD(T)/aug-cc-pVDZ levels of theory, help to verify the stability of the U(Ar) VB aG anion. At the UMP2/aug-cc-pVDZ level, the anion is adiabatically unbound with respect to the neutral by 0.073 eV. With the aug-cc-pVQZ basis set, the calculation did not converge for the anion. At the CCSD(T)/aug-cc-pVDZ level of theory, the U(Ar) aG VB anion is still adiabatically unbound with respect to the neutral by 0.036 eV. This tendency validates the existence of a stable V B anion only for the case of the U(Xe) complex, as indicated by the experiment of Hendricks *et al.*[8] Figure 9 shows the relative CCSD(T) energies of the aG canonical VB U(NG) anions with respect to the neutrals obtained with the different basis sets.

D. C5N1 Tautomers

Complexes of uracil structures known as very rare tautomers with noble-gas atoms were studied. The work of Bachorz *et al.*[20] showed the existence of an adiabatically bound VB anion of an imino-oxo tautomer of uracil. U^-_{C5N1} is more stable than the canonical neutral by 1.17 kcal/mol at the CCSD(T)/aug-ccpVDZ//UMP2/aug-cc-pVDZ level of theory. Figure 10 shows the structure of the tautomer named C5N1.

TABLE VII. U_{can}(NG) and U^-_{C5N1}(NG) MP2 and PUMP2/6-311++G**/aug-cc-pVDZ-PP total energies (a.u.).

	MP2		PUMP2		
Structure	ZPE		ZPE		$\langle s^2\rangle_{UHF}$
U(Ar)					
can G	−940.80780	−940.72069			
C5N1 aG	−940.79951	−940.71604	−940.80303	−940.71955	0.78
U(Kr)					
can G	−876.17765	−876.09077			
C5N1 aG	−876.17007	−876.08663	−876.17360	−876.08663	0.78
C5N1 aB[a]	−876.16966	−876.08623	−876.17310	−876.08967	0.78
U(Xe)					
can G	−742.27133	−742.18429			
C5N1 aG	−742.26457	−742.18112	−742.26814	−742.18469	0.78
C5N1 aB[a]	−742.26409	−742.18068	−742.26756	−742.18415	0.78

[a]Anion structure optimized from the neutral C5N1 B.

TABLE VIII. U^-_{C5N1}(NG) UMP2 and PUMP2 with 6-311++G**/aug-cc-pVDZ-PP basis set AEAs[a] (eV).

	UMP2		PUMP2	
Structure	AEA	AEA+ZPE	AEA	AEA+ZPE
U^-_{C5N1}(Ar)				
aG	−0.226	−0.127	−0.130	− 0.031
U^-_{C5N1}(Kr)				
aG	−0.206	−0.113	−0.110	− 0.017
aB[b]	−0.217	−0.121	−0.124	− 0.027
U^-_{C5N1}(Xe)				
aG	−0.184	−0.086	−0.087	0.011
aB[b]	−0.197	−0.100	−0.103	− 0.006

[a]AEAs represent the energy difference between the canonical neutrals and VB tautomeric anions.
[b]Anion structure optimized from the neutral C5N1 B which can be considered an aG structure.

The same methodology used for canonical complexes was employed in studying C5N1 tautomers complexes. However, only the B and G tautomers structures were studied, since it was shown that they were minima in the canonical complexes.

The anion structures for U^-_{C5N1}(Ar), U^-_{C5N1}(Kr), and U^-_{C5N1}(Xe) were optimized at the UMP2/6-311++G** (aug-cc-pVDZ-PP on Kr and Xe) level of theory. ZPE corrections were obtained at the same level. Only VB anions were obtained and identified as minima. Two anions were studied first, B and G. For U^-_{C5N1}(Ar), only the G structure was identified as a minimum; the B structure was identified as a transition state. For the Kr and Xe complexes, both B and G anions were found as minima. Nevertheless, the B structures converged to a geometry closer to that of the G structure than the B one. Therefore, when compared to the canonical neutral, B anions are related to the G neutral canonical complex. Table VII shows MP2 and UMP2 energies of the VB anions, compared to the energies of the respective neutral canonical structures. The total electronic energies of the aB and aG VB anions are practically the same. Since the initial geometry of the neutral B structure was used as starting point for the optimization of the VB aB anion and convergence was achieved for a structure very similar to the aG VB anion, one can assume complexes aB and aG should be considered as only one structure.

Figures 3–5 show the optimized structures of the aG VB C5N1 anions. Molecular orbital diagrams are shown in Figures 6–8. Optimized geometries of the C5N1 anions are notably different from the canonical neutrals. Both B and G Kr and Xe anionic complexes present the group C5-H_2 placed either above the uracil ring plane, nearer to the noble-gas atom, or beneath the uracil ring plane by angles that vary between 33° and 44°. Moreover, in the Ar anionic complex, the C5-H_2 group deviates from planarity by 35°. In agreement with the previous discussion for the canonical anions, those features are characteristic of VB anions. $\langle s^2\rangle_{UHF}$ values higher than 0.78 (see Table VII) also indicate the formation of VB anions.

The PUMP2 ZPE corrected energies evince the existence of an *adiabatically bound* VB U^-_{C5N1}(Xe) anion. This anion is more stable than the canonical neutral by 0.25 kcal/mol. The most stable V B U^-_{C5N1}(Ar) and U^-_{C5N1}(Kr) anions are *adiabatically unbound* with respect to the canonical neutral by 0.71 and 0.38 kcal/mol, respectively. AEA and VEDE values are shown in Tables VIII and IX.

The aG VB U^-_{C5N1}(Xe) anion presents a positive AEA value of 0.011 eV at the PUMP2 level and VEDE values of 1.25, 1.38, and 1.59 eV at the PUMP2, OVGF, and P3 levels of theory, respectively. These values are much larger than the broadband that appears in Figure 1 between 0.2 and 1.0 eV. Therefore, experimental information does not provide conclusive evidence for the presence of this tautomer, for calculated VEDEs lie in the tail of the observed spectrum.

Moreover, a second very-rare tautomer was studied. C5N3 U(NG) complexes were investigated using the same methodology used for the C5N1 tautomers. Figures 6–8 show orbital plots of the singly occupied orbitals of U(NG) aG VB anions. No DB anion was found for U(NG) C5N3 tautomers. VEDEs of 1.21, 2.50, and 2.52 eV were obtained at the UMP2/6-311++G** level of theory for U(Ar), U(Kr), and U(Xe) aG VB C5N3 anions, respectively. Since those values exceed the spectral range of the three complexes U(Ar), U(Kr), and U(Xe) and are not adiabatically bound with respect to the neutral, no further investigation on C5N3 tautomers was carried out.

TABLE IX. U^-_{C5N1}(NG) UMP2, PUMP2, OVGF, and P3 with 6-311++G**/aug-cc-pVDZ-PP basis set VEDEs (eV).

Structure	UMP2	PUMP2	OVGF	P3
U^-_{C5N1}(Ar)				
aG	1.11	1.21	1.33	1.54
U^-_{C5N1}(Kr)				
aG	1.14	1.23	1.36	1.57
aB[a]	1.12	1.21	1.35	1.55
U^-_{C5N1}(Xe)				
aG	1.15	1.25	1.38	1.59
aB[a]	1.14	1.24	1.38	1.59

[a]Anion structure optimized from the neutral C5N1 B which can be considered an aG structure.

IV. CONCLUSIONS

This study reports AEA and VEDE values for the DB and VB anions of U(Ar), U(Xe), and U(Kr) complexes obtained by UMP2, CCSD(T), OVGF, and P3 levels of theory. A VB *adiabatically bound* anion was found for the U(Xe) G complex. Negative AEAs of −0.036 and −0.020 eV were obtained at the CCSD(T)/aug-cc-pVDZ level of theory for aG VB U(Ar) and U(Kr) canonical anions. At the same level of theory, a positive AEA of 0.010 eV was obtained for the aG VB U(Xe) canonical anion. VEDEs obtained for all DB and VB complexes (see Table VI) are in excellent agreement with the experimental data. *Adiabatically bound* DB anions were characterized and assigned to sharp peaks around 0.05 eV.[8] An *adiabatically bound* VB U(Xe) anion was assigned to a broad band observed between 0.2 and 1.0 eV.[8] Moreover, an *adiabatically bound* VB very-rare tautomer anion was characterized for the U(Xe) complex, with a VEDE value over 1.0 eV (see Table IX). However, there is no conclusive evidence of its existence from experimental observations. The coexistence of DB and VB anions of the U(Xe) complex follows from the present results. For U(Ar) and U(Kr) complexes, the existence of only DB anions is predicted.

ACKNOWLEDGMENTS

The authors are grateful to the Brazilian agency FAPESP and to the National Science Foundation (NSF) (Grant No. CHE-0809199) for financial support.

[1] L. Sanche, Mass Spectrom. Rev. **21**, 349 (2002).
[2] B. Boudaiffa, P. Cloutier, D. Hunting, A. Huels, and L. Sanche, Science **287**, 1658 (2000).
[3] A. O. Colson and M. D. Sevilla, Int. J. Radiat. Biol. **67**, 627 (1995).
[4] M. Anbar and G. A. St. John, Science **190**, 781 (1975).
[5] N. A. Oyler and L. Adamowicz, J. Phys. Chem. **97**, 11122 (1993).
[6] C. Desfrançois, H. AbdoulCarime, and J. P. Schermann, J. Chem. Phys. **104**, 7792 (1996).
[7] J. H. Hendricks, S. A. Lyapustina, H. L. de Clercq, J. T. Snodgrass, and K. H. Bowen, J. Chem. Phys. **104**, 7788 (1996).
[8] J. H. Hendricks, S. A. Lyapustina, H. L. de Clercq, and K. H. Bowen, J. Chem. Phys. **108**, 8 (1998).
[9] J. Schiedt, R. Weinkauf, D. M. Neumark, and E. W. Schlag, Chem. Phys. **239**, 511 (1998).
[10] S. Eustis, D. Wang, S. Lyapustina, and K. H. Bowen, J. Chem. Phys. **127**, 224309 (2007).
[11] O. Dolgounitcheva, V. G. Zakrzewski, and J. V. Ortiz, J. Phys. Chem. **103**, 7912 (1999).
[12] J. Smets, W. J. McCarthy, and L. Adamowicz, J. Phys. Chem. **100**, 14655 (1996).
[13] C. A. Morgado, K. Y. Pichugin, and L. Adamowicz, Phys. Chem. Chem. Phys. **6**, 2758 (2004).
[14] D. Roca-Sanjuán, M. Merchán, L. Serrano-Andrés, and M. Rubio, J. Chem. Phys. **129**, 095104 (2008).
[15] R. A. Bachorz, W. Kopper, and M. Gutowski, J. Chem. Phys. **126**, 085101 (2007).
[16] H. Motegi and T. Takayanagi, J. Mol. Struct.: THEOCHEM **907**, 85 (2009).
[17] P. Dedíková, P. Neogrády, and M. Urban, J. Phys. Chem. A **115**, 2350 (2011).
[18] X. Li, Z. Cai, and M. D. Sevilla, J. Phys. Chem. A **106**, 1596 (2002).
[19] A. F. Jalbout, K. Y. Pichugin, and L. Adamowicz, Theor. Chem. Acc. **111**, 358 (2004).
[20] R. A. Bachorz, J. Rak, and M. Gutowski, Phys. Chem. Chem. Phys. **7**, 2116 (2005).
[21] M. Haranczyk and M. Gutowski, J. Am. Chem. Soc. **127**, 699 (2005).
[22] K. Mazurkiewicz, M. Haranczyk, M. Gutowski, J. Rak, D. Radisic, S. N. Eustis, D. Wang, and K. H. Bowen, J. Am. Chem. Soc. **129**, 1216 (2007).
[23] J. V. Ortiz, Adv. Quantum Chem. **35**, 33 (1999).
[24] J. V. Ortiz, in *Computational Chemstry: Reviews of Current Trends* (World Scientific, Singapore, 1997), Vol. 2, p. 1.
[25] M. J. Frisch, G. W. Trucks, and H. B. Schlegel *et al.*, GAUSSIAN 09, Revision B.01, Gaussian, Inc., Wallingford, CT, 2010.
[26] V. G. Zakrzewski and J. V. Ortiz, Int. J. Quantum Chem. **S28**, 23 (1994).
[27] V. G. Zakrzewski and J. V. Ortiz, Int. J. Quantum Chem. **53**, 583 (1995).
[28] V. G. Zakrzewski, O. Dolgounitcheva, A. V. Zakjevskii, and J. V. Ortiz, Annu. Rev. Comput. Chem. **6**, 79 (2010).
[29] J. Schirmer, L. S. Cederbaum, and O. Walter, Phys. Rev. A **28**, 1237 (1993).
[30] W. von Niessen, J. Schirmer, and L. S. Cederbaum, Comput. Phys. Rep. **1**, 57 (1984).
[31] V. G. Zakrzewski, O. Dolgounitcheva, and J. V. Ortiz, Int. J. Quantum Chem. **75**, 607 (1999).
[32] V. G. Zakrzewski, O. Dolgounitcheva, and J. V. Ortiz, Int. J. Quantum Chem. **80**, 836 (2000).
[33] K. A. Peterson, D. Figgen, E. Goll, H. Stoll, and M. Dolg, J. Chem. Phys. **119**, 11113 (2003).
[34] T. H. Dunning, Jr., J. Chem. Phys. **90**, 1007 (1989).
[35] D. E. Woon and T. H. Dunning, Jr., J. Chem. Phys. **98**, 1358 (1993).
[36] G. Schaftenaar and J. H. Noordik, J. Comput.-Aided Mol. Des. **14**, 123 (2000).
[37] Y. Öhrn and G. Born, Adv. Quantum Chem. **13**, 1 (1981).